M. W. Brown and D. E. Buckthorpe†*

A Crack Propagation Based Effective Strain Criterion

REFERENCE Brown, M. W. and Buckthorpe, D. E., **A crack propagation based effective strain criterion**, *Biaxial and Multiaxial Fatigue*, EGF 3 (Edited by M. W. Brown and K. J. Miller), 1989, Mechanical Engineering Publications, London, pp. 499–510.

ABSTRACT Codes for design against fatigue invariably describe failure as a crack initiation process, as may be characterised by a uniaxial strain/life curve. When multiaxial strains are induced in engineering components, they can be related by an effective strain formula to the uniaxial curve, this formula being couched in terms of the principal strains applied. However, fundamental studies of the fatigue process show that it is one of crack propagation, which implies that the most suitable effective strain criteria should take account of the two basic propagation phases, Stage I and Stage II crack growth. A new formula is proposed, which is compared to available experimental data for both proportional and out-of-phase multiaxial loading.

Introduction

An indispensable aspect of any fatigue design code concerned with finite lifetimes is the treatment of multiaxial cyclic strains. Since the allowable cyclic strain range for design purposes is generally based on empirical data for a given material, temperature, and environment, the designer must relate such data to the actual multiaxial cyclic strains extant in a component. Invariably the material data are generated with the uniaxial stress state, i.e., using push–pull, rotating bending, or cantilever bending tests. Therefore, most design guidelines have been based on the reduction of a multiaxial cyclic strain situation to an equivalent uniaxial strain range, from which a life estimate can be made.

An important example (**1**) is the octahedral equivalent strain range, which is based on the effective strain employed in plasticity theory and the Prandtl–Reuss equations (**2**). In terms of principal strains, ε_1, ε_2, and ε_3, this may be written as

$$\Delta\varepsilon_{eq_M} = \frac{1}{\sqrt{2}(1+\nu)} \{(\Delta\varepsilon_1 - \Delta\varepsilon_2)^2 + (\Delta\varepsilon_2 - \Delta\varepsilon_3)^2 + (\Delta\varepsilon_3 - \Delta\varepsilon_1)^2]^{1/2} \quad (1)$$

where ν is the elasto-plastic value of Poisson's ratio, and Δ represents the range of strain. In reference (**1**), ν is taken to be 0.5. Clearly equation (1) can be associated with the von Mises yield criterion, for a strain level equal to cyclic

* Department of Mechanical Engineers, University of Sheffield, Mappin Street, Sheffield, S1 3JD, UK.
† National Nuclear Corporation, Warrington Road, Risley, Warrington, WA3 6BZ, UK.

yield. Another equivalent strain formula is based on the Tresca or maximum shear criterion (3), giving

$$\Delta\varepsilon_{eq_T} = \frac{1}{(1+\nu)}(\Delta\varepsilon_1 - \Delta\varepsilon_3) \tag{2}$$

where $\varepsilon_1 \geq \varepsilon_2 \geq \varepsilon_3$, ε being the cyclic strain amplitude.

These definitions of equivalent strain are in stark contrast to the implications of linear elastic fracture mechanics (LEFM), on which defect tolerant design codes will inevitably be based. In situations where LEFM is applicable, cracks are observed to follow the opening mode, the crack path being normal to the maximum principal stress. This is true for both ductile and brittle materials in low stress situations (stress well below yield), the rate of crack propagation being determined by the stress intensity factor, K, through relationships such as the Paris law

$$\frac{da}{dN} = C(\Delta K)^m \tag{3}$$

where C and m are material constants. Thus LEFM suggests that the maximum principal stress range is a fundamental parameter in determining fatigue life, because all fatigue failures are caused by the development of cracks throughout a components lifetime. It should be noted that all mode I stress intensity factors may be written as (4)

$$K = Y\sigma_1\sqrt{(\pi a)} \tag{4}$$

where Y is a factor dependent on geometry alone, and σ_1, is the stress normal to the crack of length, a.

This paper re-assesses the equivalent strain concept in the light of current knowledge concerning the behaviour of fatigue cracks. An equivalent strain formula is derived from a simplified analysis of Stage I and II crack propagation in smooth specimens and is then compared to published experimental data.

Notation

A	Weighting function
a	Crack length
b	Bending fatigue strength
C	Constant
E	Young's modulus
G	Modulus of rigidity
K	Stress intensity factor
k	Cyclic strength coefficient
m	Constant
N	Number of cycles
n	Cyclic strain hardening exponent

Q	t/b
R	Ratio of minimum and maximum loads
t	Torsional fatigue strength
Y	Geometry factor
γ	Shear strain amplitude
Δ	Range
ε	Normal strain amplitude
λ	$\Delta\gamma/\Delta\varepsilon$, biaxiality factor
ν	Poisson's ratio
σ	Normal stress
τ	Shear stress

Subscripts

C	Crack propagation equivalent strain
e	Elastic
eq	Equivalent strain
fl	Fatigue limit
M	von Mises
max	Maximum shear value
O	Material constant
P	Plastic
R	Rankine
s	Secant modulus
T	Tresca
yield	Yield stress
1, 2, 3	Principal values
I	Stage I
II	Stage II

Equivalent strain criteria

Equations (1) and (2) define the two most widely used equivalent strain criteria, both of which are based on monotonic yield criteria on the assumption that fatigue is governed primarily by deformation processes. Due to the lack of success of these equations in correlating empirical fatigue data, a number of formulae for a fatigue equivalent strain have been proposed, which are adequately reviewed elsewhere (5)–(7). Most approaches require one or two material constants to be incorporated in the equivalent strain to provide an adequate fit to observed behaviour. This implies that data from more than one multiaxial stress state are necessary to derive the equivalent strain, which is a serious shortcoming for the designer who generally has only uniaxial results available.

An example for high cycle fatigue behaviour is given by McDiarmid (8), where a term $Q = t/b$ is introduced into the relationship for allowable surface strain amplitudes. Here t is the torsional fatigue strength and b is the bending

fatigue strength at the fatigue limit. A compilation of values for t/b can be found in Forrest (**9**).

Two examples of low cycle fatigue criteria are based on linear (**10**) and quadratic (**11**)(**12**) relationships using shear and normal strains, respectively, similar to the expressions first proposed by Gough *et al.* (**13**) in stress terms for high cycle fatigue. Each case involves the fitting of the equivalent strain formula to two strain–life curves, one for uniaxial push–pull or reversed bend tests and a second for reversed torsion. Although good correlation of low cycle fatigue data is achieved by such methods, the approach developed in this paper uses only the uniaxial curve and a single value, $Q = t/b$, to characterize the multiaxial fatigue response. This should minimise the additional data required over and above the present fatigue data base available to the designer.

Phases of fatigue crack growth

There are two dominant phases of fatigue crack growth, termed Stage I and Stage II by Forsyth (**14**). Stage I is a shear mode of growth which extends for one or two grains from the point of crack initiation. Stage II follows and, being normal to the maximum principal stress (or strain), it exhibits mode I crack opening and generally produces a fracture surface characterised by striations.

Stage I cracking is observed to play a significant role in long life or high cycle fatigue (**15**), whereas at higher strain ranges (low cycle fatigue) the majority of the fracture surface of a failed specimen shows Stage II failure. The relative proportions of Stages I and II depend on the number of cycles to failure (**15**). Stage I, being a shear mechanism and limited to the first one or two grains, is readily identified with microstructurally short cracks (**16**). These are currently receiving considerable attention since they do not obey the rules of conventional fracture mechanics. Cracks form on persistent slip bands or grain boundaries, always aligned with planes that experience maximum shear deformation. Thus, one might expect a Tresca criterion to correlate the maximum shear strain, which provides the driving force for microstructurally short cracks. A study of short cracks in a medium carbon steel subjected to tensile and torsional strain cycles, respectively, confirmed that the Tresca criterion showed a satisfactory correlation of crack growth rates (**17**). Thus the relevant equivalent strain is given by equation (2), noting that shear stress and shear strain are uniquely linked through the cyclic stress–strain curve (**18**), for ductile metals.

Stage II cracking bears all the characteristics of mode I LEFM crack behaviour. Therefore one might reasonably expect the maximum principal stress to correlate crack growth rate, since this determines the stress intensity factor, equation (4). This indicates the importance of the Rankine failure criterion, which has been confirmed by biaxial fatigue studies in the low stress regime (**19**), where $\sigma_{max} \ll \sigma_{yield}$. Even where the stress amplitudes approach the yield stress, the normal stress on a crack has been observed to be the most

important parameter determining crack propagation rate (**20**). For elastic conditions, the maximum principal stress is given by

$$\sigma_1 = E\{\varepsilon_1(1 - 2\nu_e) + \nu_e(\varepsilon_1 + \varepsilon_2 + \varepsilon_3)\}/\{(1 + \nu_e)(1 - 2\nu_e)\} \quad (5)$$

where E and ν_e are Young's modulus and the elastic Poisson's ratio. For proportional loading conditions, equation (6), may be extended to elastic–plastic conditions by replacing E with the secant modulus, E_s, and ν_e with the elasto–plastic Poisson's ratio, ν. Thus an equivalent strain may be defined, equal to σ_1/E_s, where

$$\varepsilon_{eq_R} = \frac{1}{(1 + \nu)}\{\varepsilon_1 + (\varepsilon_1 + \varepsilon_2 + \varepsilon_3)\nu/(1 - 2\nu)\} \quad (6)$$

The correlation of LEFM crack propagation data by the strain σ_1/E for a wide range of metals has been observed previously by Frost *et al.* (**21**), who show that mode I crack growth data fall into a narrow band when plotted against $\Delta K/E$. So the use of equation (6) to correlate the growth of long cracks should find general applicability.

The first phase of fatigue life, crack initiation, occurs very rapidly when compared to the Stage I growth period, even in high cycle fatigue close to the fatigue limit (**16**). Similarly, the final phase of ductile crack growth, or Stage III, occupies a negligible fraction of the overall endurance. Thus, in life assessment and the definition of an equivalent fatigue strain, the endurance can be divided into two significant periods, (a) Stage I, which takes equation (2) for an equivalent strain, and (b) Stage II, for which equation (6) is the equivalent strain. Equation (2) may be re-written as an amplitude to enable direct comparison with equation (6)

$$\varepsilon_{eq_T} = \frac{1}{(1 + \nu)}(\varepsilon_1 - \varepsilon_3) \quad (7)$$

where $\varepsilon_1 \geqslant \varepsilon_2 \geqslant \varepsilon_3$, and ε_1 is the greatest principal strain amplitude in the surface plane of a biaxially stressed component. Note that equations (6) and (7) have been derived for the case of fully reversed strain controlled cycling.

A crack propagation based equivalent strain

Since fatigue life consists of two stages of crack growth, governed by the equivalent strains of equations (7) and (6), respectively, the overall effective strain for fatigue should combine these two equations in proportions given by the number of cycles spent in Stages I and II, respectively. Thus one may define an equivalent strain

$$\varepsilon_{eq_C} = A\varepsilon_{eq_R} + (1 - A)\varepsilon_{eq_T} \quad (8)$$

where the weighting function $A = N_{II}/(N_I + N_{II})$. Here N_{II} is the number of

cycles spent in Stage II and N_I is the number of cycles in Stage I, together with any transition.

Now, in high cycle fatigue, A will take a low value to favour the Tresca criterion for Stage I cracking, but as the applied strain range is increased, A will increase, approaching unity for low cycle, high-strain fatigue situations. Thus, A may be taken as a function of endurance, or alternatively an equivalent but more convenient form for A depends on strain amplitude. Fatigue is strongly dependent on cyclic plasticity, and plastic deformation is, of course, related to the Tresca equivalent strain directly (**18**). We, therefore, postulate the weighting function

$$A = 1 - \sqrt{(\varepsilon_O/\varepsilon_{eq_T})} \tag{9}$$

which has been chosen to give conservative life predictions for the experimental data presented in the following section. The strain ε_O is a material constant, which may be related to the uniaxial fatigue limit, ε_{fl} and Q, the t/b ratio.

For combined tension–torsion loading, equation (7) becomes

$$\varepsilon_{eq_T} = \sqrt{\{\varepsilon^2 + \gamma^2/(1 + \nu)^2\}} \tag{10}$$

and equation (6) becomes

$$\varepsilon_{eq_R} = (\varepsilon_{eq_T} + \varepsilon)/2 \tag{11}$$

where ε and γ are the axial and torsional strain amplitudes. Correlating equation (8) with the uniaxial fatigue limit at high cycles and putting $\varepsilon = b/E$ and $\gamma = t/G$, where

$$G = E/\{2(1 + \nu_e)\}$$

after some algebra, one obtains

$$\varepsilon_O = (1/Q - 1)^2 \cdot 2Q\varepsilon_{fl} \tag{12}$$

since

$$\varepsilon_{fl} = b/E$$

Thus to derive the equivalent strain ε_{eq_C}, the only material data required are the uniaxial fatigue limit amplitude, ε_{fl}, and the value of $Q = t/b$. The value of ε_{fl} comes from the uniaxial strain–life curve.

Correlation of experimental data

In order to evaluate the effectiveness of the equivalent strain in equation (8), three sets of data for different materials have been considered.

Firstly, results have been published for austenitic stainless steels at ambient temperature by Sonsino and Grubisic (**22**) and Moguerou *et al.* (**23**) using Type 321 and 316 steels, respectively. Using fatigue limits from NRIM data sheets (**24a**)–(**24b**), the results are plotted for ε_{eq_C} in Fig. 1, together with results for

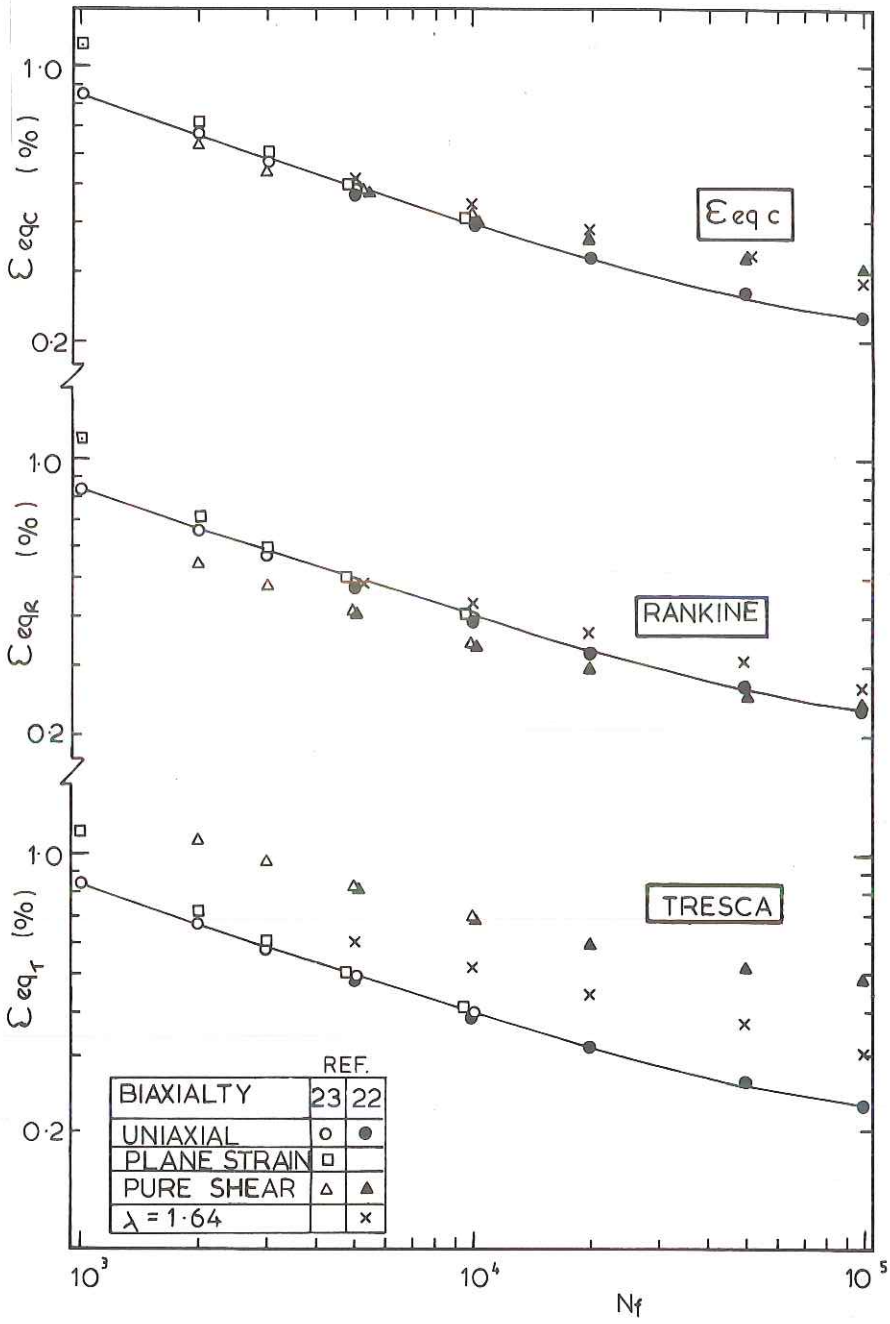

Fig 1 Correlation of fatigue data for type 316 and 321 stainless steels by: (a) crack propagation equivalent strain, (b) Rankine equivalent strain, (c) Tresca equivalent strain (22)(23)

Table 1 Material properties employed in the analysis

Material	*316, 321 stainless steel*	*316 stainless steel*	*1% Cr–Mo–V steel*
Temperature (°C)	20	400	20
k (*MPa*)	1014	1623	1056
n	0.199	0.242	0.085
E (*GPa*)	198	167.3	208
ν_e	0.29	0.322	0.29
Q	0.693	0.693	0.60
ε_{fl} (%)	0.115	0.155	0.193
ε_O (%)	0.0313	0.0422	0.103
References	**(22)(23)(24a,b)**	**(11)(18)(24a,b)**	**(11)(18)(25)**

the Tresca and Rankine equivalent strains for comparison. The material data used in the equations are listed in Table 1. It is apparent that equation (8) gives a significant improvement over the traditional Tresca equivalent strain, and is more conservative than the Rankine equivalent strain compared to the uniaxial line.

In order to evaluate the elasto–plastic Poisson's ratio in the derivation of Fig. 1, the multiaxial form of the cyclic stress strain curve was taken from the maximum shear stress and strain (**18**),

$$\tau_{\max} = (k/2)(\gamma_{\text{pmax}}/1.5)^n \tag{13}$$

where γ_{pmax} is the maximum plastic shear strain amplitude, k is the uniaxial cyclic strength coefficient, and n is the cyclic strain hardening exponent. Then Poisson's ratio is given by (**1**)

$$\nu = 0.5 - (0.5 - \nu_e)/(1 + E\varepsilon_p^{(1-n)}/k) \tag{14}$$

where the equivalent plastic strain, ε_p, is given by $\gamma_{\text{pmax}}/1.5$.

Secondly, results are shown in Fig. 2 for a Type 316 austenitic stainless steel at 400°C, in combined tension–torsion tests (**11**). A clear trend can be observed with biaxiality, λ, where $\lambda = \Delta\gamma/\Delta\varepsilon$, for this material which exhibited a degree of anisotropy. In the derivation of equations (8), (9), and (12), isotropic material properties were implicitly assumed, and, therefore, a divergence in experimental results is to be expected for any anisotropic metal.

Thirdly, a bainitic 1% Cr–Mo–V steel has been examined in low cycle fatigue for both proportional and non-proportional loading (**11**)(**25**)–(**27**). Since no fatigue limit data were available for this material, the value of Q was assumed to be 0.6, a typical value predicted by the von Mises criterion (**9**). The uniaxial fatigue strength was estimated as one half of the tensile strength. Even with these simple assumptions for the derivation of ε_O, the low cycle fatigue behaviour shows a conservative correlation of data, generally within a factor of 2 on life, for the proportional loading data in Fig. 3. Note that the solid points plotted correspond to repeated strain cycling ($R = 0$), whereas the open points show fully reversed strain controlled results ($R = -1$).

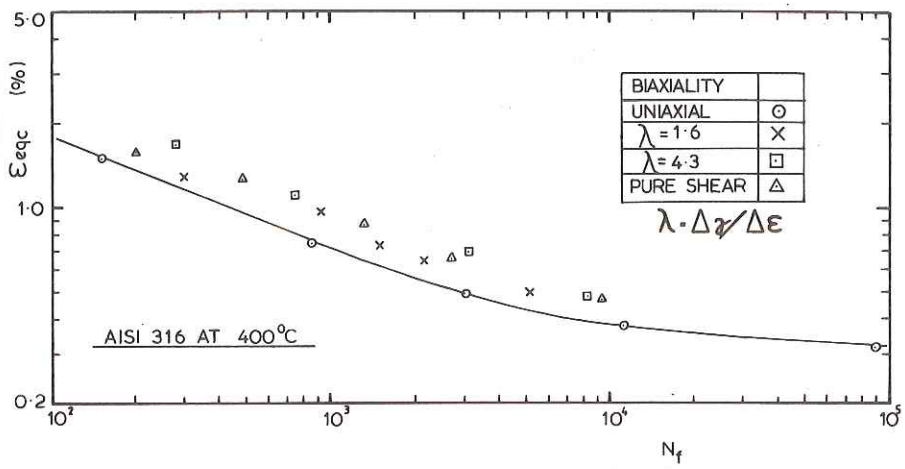

Fig 2 Correlation of tension–torsion fatigue results for type 316 stainless steel at 400°C (11)

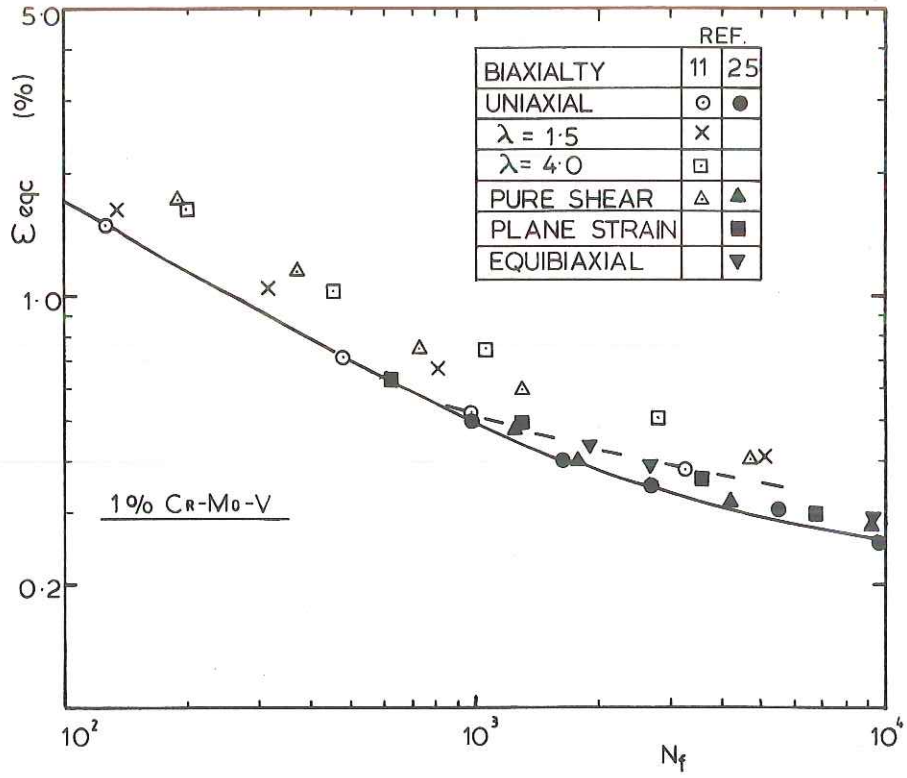

Fig 3 Correlation of data for 1% Cr–Mo–V steel under proportional loading with triangular waveform (11)(25)

For non-proportional loading, the analysis of fatigue behaviour is complex (7). Although systematic analysis of stress–strain behaviour can be accomplished, there is no generally agreed method for relating fatigue endurance to applied strains. However, in low cycle fatigue, reduced lifetimes are found where rotation of principal axes of strain occurs during a cycle (**26**). Therefore, a simple design rule is suggested, that the out-of-phase applied strain amplitudes should be treated as if they were in-phase, in order to obtain an artificially high value of equivalent strain, ε_{eq_C}. There is no physical justification for such a procedure, as strains of the calculated magnitude never arise at any time during the cycle. Its value lies in its simplicity of application, and in its ability to represent actual behaviour. This procedure has already been employed in high cycle fatigue, demonstrating a conservative tendency (**28**), and Fig. 4 shows low cycle fatigue results for the bainitic Cr–Mo–V steel. The conservative nature of the method disappears at low lives, but, nevertheless, lives are within a factor of 2 of the equivalent strain–life relationship.

In Figs 1–4, the lines drawn are fitted to the uniaxial results alone, since these are generally the material data available to the designer.

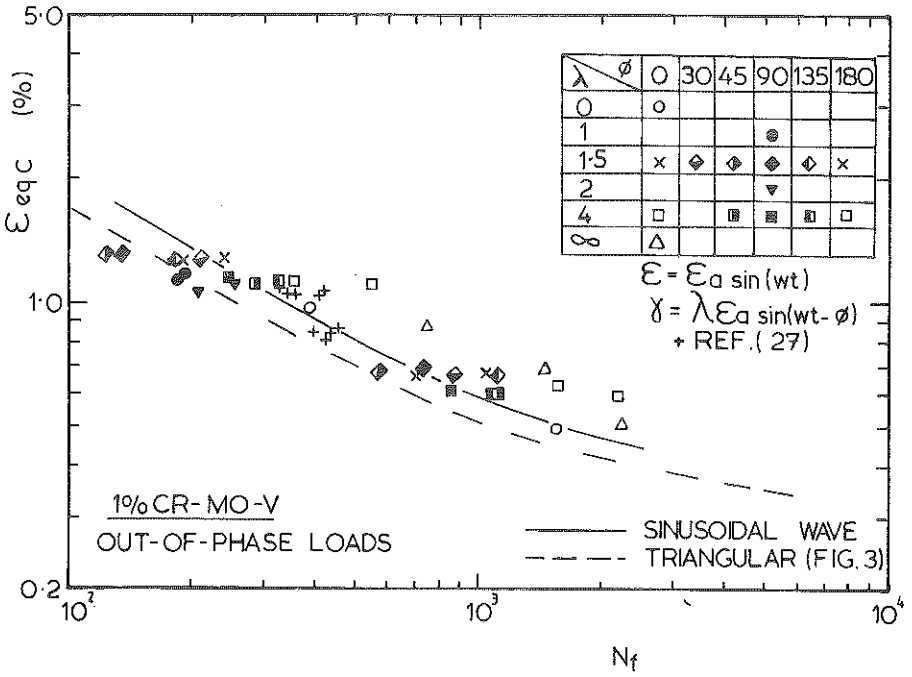

Fig 4 Correlation of data for 1% Cr–Mo–V steel under non-proportional loading with sinusoidal waveform (26) and complex strain cycles (27). The dashed line corresponds to the uniaxial data of Fig. 3, where a triangular waveform was used

Discussion

Satisfactory correlation of experimental results with the proposed equivalent strain criterion has been demonstrated for three sets of experimental data in low cycle fatigue. Good correlation of high cycle fatigue data is ensured by fitting the formula for ε_{eq_C} to the fatigue limits in tension and torsion (8) through equation (12). This new criterion differs from most previous formulae because: (a) it combines both low and high cycle fatigue behaviour, (b) it is based on considerations of actual fatigue mechanisms, (c) a minimal amount of multiaxial data is required (being the ratio Q alone).

Equations (6)–(8) have been derived from observation of fatigue crack propagation behaviour. The use of equation (9) provides the only means for fitting empirical multiaxial fatigue results. Other forms for equation (9) could be considered, for example

$$A = 1 - \varepsilon_O/\varepsilon_{eq_T}$$

which gives the corresponding material constant

$$\varepsilon_O = 2(1 - Q)\varepsilon_{fl}$$

This formula for A gives lower values for equivalent strain, and data correlation is still good although less conservative than the results in Figs 1–4.

In practice, the full evaluation of ε_{eq_C} is frequently not necessary. If ε_{eq_T} is determined initially, equation (7), and if ε_{eq_T} gives a satisfactory design life on the strain–life curve, no further analysis is necessary. The evaluation of ε_{eq_R} and, hence, ε_{eq_C} can only extend the allowable life, as ε_{eq_T} is an upper bound solution for strain. Secondly, for stress states in the first and third quadrants of biaxial stress space, ε_{eq_C}, ε_{eq_T}, and ε_{eq_R}, are identical, so only ε_{eq_T} needs to be determined. So in the majority of cases, the Tresca failure criterion is a sufficient condition for assessment of a multiaxial cyclic strain state.

Conclusions

(1) Multiaxial fatigue life can be assessed in terms of two phases of crack propagation, Stage I and Stage II.
(2) A new equivalent strain criterion is proposed for fatigue, based on crack propagation mechanics.
(3) A simple method is proposed for treating non-proportional loading in design assessments.
(4) Both low and high cycle fatigue behaviour are encompassed by a single equivalent strain criterion.

References

(1) AMERICAN SOCIETY OF MECHANICAL ENGINEERS (ASME) (1977), *Boiler and pressure vessel code*, Section XI, Code Case N-47-12.
(2) HILL, R. (1950) *The mathematical theory of plasticity*, Oxford University Press, Oxford, pp. 38–45.
(3) ASME (1977) *Boiler and pressure vessel code*, Section III.

(4) PARIS, P. C. and SIH, G. C. (1970) Stress analysis of cracks, in *ASTM STP 381*, ASTM, Philadelphia, PA, pp. 30–83.
(5) GARUD, Y. S. (1981) Multiaxial fatigue: a survey of the state of the art, *J. Testing Evaluation*, **9**, 165–178.
(6) BROWN, M. W. and MILLER, K. J. (1982) Two decades of progress in the assessment of multiaxial low cycle fatigue life, in *ASTM STP 770*, ASTM, Philadelphia, PA, pp. 482–499.
(7) MILLER, K. J. and BROWN, M. W. (Editors) (1985) *Multiaxial Fatigue, ASTM STP 853*, ASTM, Philadelphia, PA.
(8) McDIARMID, D. L. (1985) Designing for high-cycle biaxial fatigue using surface strain records, in *ASTM STP 853*, ASTM, Philadelphia, PA, pp. 431–439.
(9) FORREST, P. G. (1962) *Fatigue of Metals*, Pergamon Press, Oxford, pp. 108–113.
(10) SOCIE, D. F., WAILL, L. A., and DITTMER, D. F. (1985) Biaxial fatigue of Inconel 718 including mean stress effects, in *ASTM STP 853*, ASTM, Philadelphia, PA, pp. 463–481.
(11) BROWN, M. W. and MILLER, K. J. (1979) High temperature low cycle biaxial fatigue of two steels, *Fatigue Engng Mater. Structures*, **1**, 217–229.
(12) KANDIL, F. A., MILLER, K. J., and BROWN, M. W. (1985) Creep and ageing interactions in biaxial fatigue of type 316 stainless steel, in *ASTM STP 853*, ASTM, Philadelphia, PA, pp. 651–668.
(13) GOUGH, H. J., POLLARD, H. V., and CLENSHAW, W. J. (1951), *Some experiments on the resistance of metals to fatigue under combined stresses* (Aero. Res. Council, Rep. Memo 2522), HMSO, London.
(14) FORSYTH, P. J. E. (1961) A two stage process of fatigue crack growth, *Proc. Crack Propagation Symposium*, Cranfield, UK, pp. 76–94.
(15) WAREING, J. (1983) Mechanisms of high temperature fatigue and creep–fatigue failure in engineering materials, *Fatigue at High Temperature* (Edited by SKELTON, R. P.), Applied Science, London, Ch. 4.
(16) BROWN, M. W. (1986) Interfaces between short, long, and non-propagating cracks, in *The Behaviour of Short Fatigue Cracks* (EGF1) (Edited by MILLER, K. J. and BROWN, M. W.), Mechanical Engineering Publications, London, pp. 423–439.
(17) PEREZ CARBONELL, E. and BROWN, M. W. (1985) A study of short crack growth in torsional low cycle fatigue for a medium carbon steel, *Fatigue Fracture Engng Mater. Structures*, **9**, 15–33.
(18) BROWN, M. W. and MILLER, K. J. (1979) Biaxial cyclic deformation behaviour of steels, *ibid.*, **1**, 93–106.
(19) KITAGAWA, H., YUUKI, R., TOHGO, K., and TANABE, M. (1985) ΔK–dependency of fatigue growth of single and mixed mode cracks under biaxial stress, in *ASTM STP 853*, ASTM, Philadelphia, PA, pp. 164–183.
(20) BROWN, M. W. and MILLER, K. J. (1985) Mode I fatigue crack growth under biaxial stress at room and elevated temperatures, *ibid.*, pp. 135–152.
(21) FROST, N. E., MARSH, K. J., and POOK, L. P. (1974) *Metal fatigue*, Oxford University Press, Oxford, pp. 245–260.
(22) SONSINO, C. M. and GRUBISIC, V. (1985), Fatigue behaviour of cyclically softening and hardening steels under multiaxial elastic–plastic deformation, in *ASTM STP 853*, ASTM, Philadelphia, PA, pp. 586–605.
(23) MOGUEROU, A., VASSAL, R., VESSIERE, G., and BAHAUD, J. (1982) Low cycle fatigue under biaxial strain, in *ASTM STP 770*, ASTM, Philadelphia, PA, pp. 519–546.
(24a) Fatigue Data Sheet No. 33 (1983) *Fatigue properties of SUS 304 (18Cr–8Ni) stainless steel bars for machine structural use*, National Research Institute for Metals, Tokyo, Japan.
(24b) Data Sheets on Elevated Temperatures No. 15 (1979) *High cycle and low cycle fatigue properties of SUS 316-HP (18Cr–12Ni–2Mo) hot rolled steel plate*, National Research Institute of Metals, Tokyo, Japan.
(25) LOHR, R. D. and ELLISON, E. G. (1980) Biaxial high strain fatigue testing of 1 Cr–Mo–V steel, *Fatigue Engng Mater. Structures*, **3**, 19–37.
(26) KANAZAWA, K., MILLER, K. J., and BROWN, M. W. (1977) Low cycle fatigue under out-of-phase loading conditions, *Trans ASME, J. Engng Mater. Technol.*, **99**, 222–228.
(27) JORDAN, E. H., BROWN, M. W., and MILLER, K. J. (1985) Fatigue under severe non-proportional loading, in *ASTM STP 853*, American Society for Testing and Materials, Philadelphia, PA, pp. 569–585.
(28) LITTLE, R. E. (1969), A note on the shear stress criterion for fatigue failure under combined stress, *Aeronaut. Q.*, **20**, 57–60.